2017

The Novel Characterization of Extracellular Vesicles Containing Proteins Which Have Been Implicated in the Pathogenesis of HIV Associated Neurocognitive Disorders

Grace Ispas
Loyola University Chicago

LOYOLA UNIVERSITY CHICAGO

THE NOVEL CHARACTERIZATION OF EXTRACELLULAR VESICLES CONTAINING PROTEINS WHICH HAVE BEEN IMPLICATED IN THE PATHOGENESIS OF HIV ASSOCIATED NEUROCOGNITIVE DISORDERS

A THESIS SUBMITTED TO

THE FACULTY OF THE GRADUATE SCHOOL

IN CANDIDACY FOR THE DEGREE OF

MASTER OF SCIENCE

PROGRAM IN INFECTIOUS DISESASE AND IMMUNOLOGY

BY

GRACE ISPAS

CHICAGO ILLINOIS

DECEMBER 2017

TABLE OF CONTENTS

LIST OF FIGURES

CHAPTER ONE

REVIEW OF THE LITERATURE

Human Immunodeficiency Virus I

Human Immunodeficiency Virus type 1 (HIV-1) was first discovered to cause Acquired Immune Deficiency Syndrome (AIDS) in 1983 and since then, continues to be a serious health issue in many parts of the world, particularly Sub-Saharan Africa and the Americas (26). Historically about 35 million people have died resulting in an HIV related illness and 70 million people have been infected with the virus. Today, an estimated 36.7 million people are living with HIV, with approximately 2.1 million new cases annually (27).

HIV-1 is known to infect CD4+ T cells, macrophages and microglial cells of the immune system. Both CD4+ T cells and macrophages express the CD4 molecule on their cell surface, as well as the chemokine receptor CCR5, both of which are utilized by HIV-1 for cellular entry. Viral binding and entry is the first step in the viral lifecycle (4, 5). The sequential binding of viral protein gp120 to both CD4 and CCR5 initiates fusion of the virus and plasma membranes, as the virus is brought in close proximity to the target cell. Following fusion, the viral core trafficks through the cytoplasm, during which time the virus begins reverse transcribing its RNA genome into the double stranded DNA form that it ultimately integrated into the host cell genome via the viral protein Integrase (4, 5). Upon integration, transcription results in the early synthesis of regulatory HIV-1 proteins, of which assist in generating longer RNA transcripts. Subsequently,

these newly structured proteins are assembled at the cell surface and released as a new, mature virion following its budding from the host cell plasma membrane (4, 5).

The pathogenesis of HIV-1 infection is a consequence of both the infecting virus, as well as the host's immune response to the virus. Viral transmission requires direct exposure and is highly dependent on the virus isolate, its concentration and host susceptibility. CD4+ T cells are the first to become infected, spreading the virus into the regional lymph nodes and subsequently into the bloodstream (4, 5). Viral replication is at its height during this acute phase of the primary infection; virus particles can be found in dendritic cells, CD4+ T cells and macrophages. Infected cells typically succumb to the infection, undergoing cell death or establishing a form of latent infection. During this stage of infection, the number of CD4+ T cells dramatically declines as viral titers rapidly increase, yet this response is short lived as the host generates humoral and cellular immune responses (4, 5). Upon Antibody-Dependent Cellular Cytotoxicity, mediated by Natural Killer T cells and HIV-specific T cells and antibodies, HIV-1 RNA levels decline and CD4+ T cells raise again, although never fully recovering from the persistent infection. The HIV-1 pathogenic effects persist, albeit asymptomatic, resulting in the progressive loss of CD4+ T cells and viral spread within the lymphoid environments. In the absence of treatment, patients develop AIDS and typically succumb to opportunistic infections due to their weakened immune system (Figure 1).

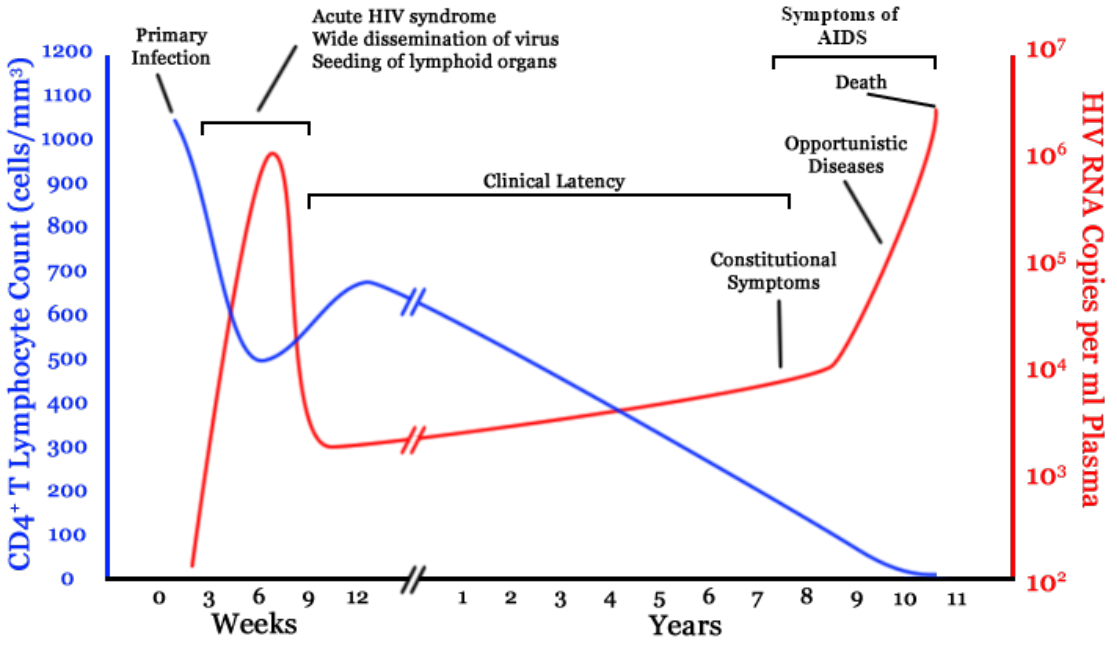

Figure 1. Treatment-Naïve HIV-1 Time Course. A schematic of treatment-naive HIV-1 infection time course in which viral RNA copies are represented in red and CD4+ T cell count in blue. HIV-1 RNA copies are steadily increasing, while CD4+ T cells are rapidly declining during the stage of primary infection. As time progresses latent reservoirs are established resulting in clinical latency. With a lack of treatment, opportunistic infections arise and HIV-1 disease will progress into AIDS.

In the past 20 years, HIV-1 infection has transitioned from a life-limiting disease often met with fatal opportunistic infections to a manageable chronic infection with a near-normal life span and few opportunistic infections. This transition has been made possible through four major advancements both in the patient care, as well as scientific research advancements including: gaining a better understanding of HIV-1 replication and the subsequent relationship of immunological and clinical progression, the development and utilization of combination antiretroviral therapy (CART), the ability to optimize patient treatment via reliable measurements of CD4+ helper T cells, plasma HIV-1 RNA levels and antiretroviral resistance

profiles, and lastly the shift of treatment with beginning CART upon HIV-1 infection and patient commitment regardless of CD4+ T cell count (26, 27).

CART works to limit HIV-1 viral replication through inhibition of multiple stages in the HIV-1 life cycle (Figure 2). Specifically, nucleoside and nucleotide reverse transcriptase inhibitors suppress viral replication, integrase inhibitors work by blocking the incorporation of the viral genome into host DNA, and protease inhibitors prevent the proteolytic cleavage of protein precursors required for the production of viral particles (4, 5). Combination therapies are advantageous in that they greatly decrease the risk of the evolution of drug-resistant strains. Unfortunately, in 2016 it was estimated that only 17 million, or about 46% of the 36.7 million individuals living with HIV-1, were actually receiving CART (26, 27).

While CART has significantly reduced the mortality associated with HIV-1, these therapies are unable to completely eradicate the infection. This is because HIV-1 is capable of establishing latency, primarily within infected CD4+ T cells, creating what are known as latent reservoirs throughout the body (4, 5). If CART is stopped or temporarily interrupted, the virus can rapidly rebound, viral replication will resume and lead to AIDS if treatment is not resumed. Furthermore, patients on CART are at an increased risk for a number of inflammatory complications, including, cardiovascular disease, renal complications and HIV-Associated Neurocognitive Disorders.

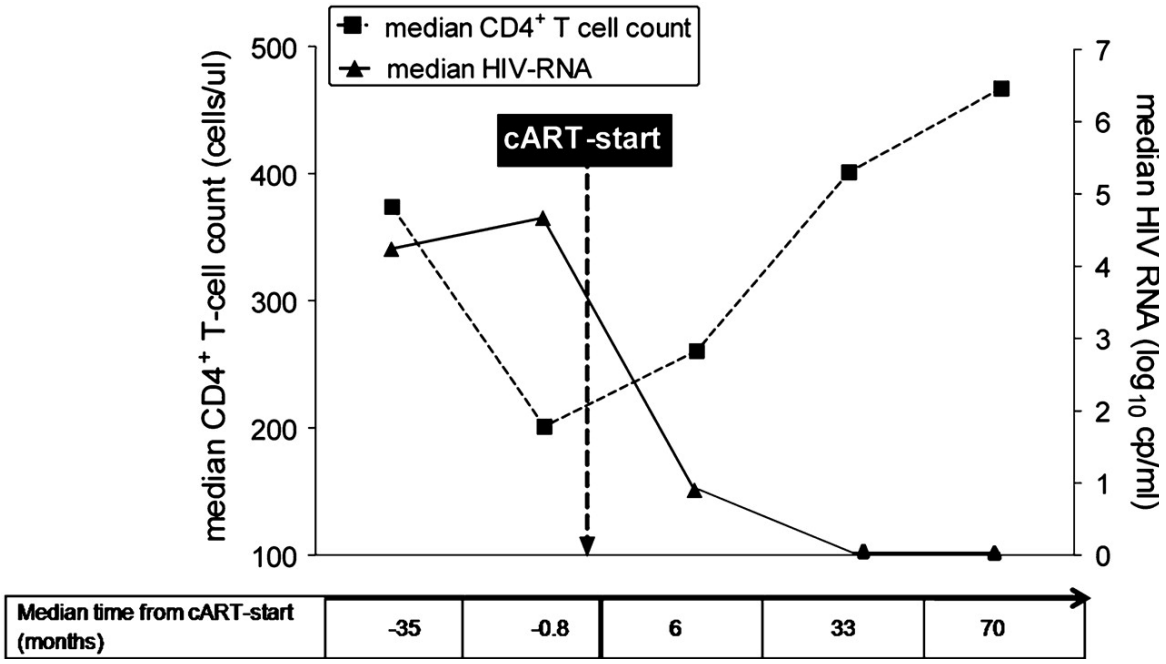

Figure 2. HIV-1 Time Course Following CART Treatment. A schematic of HIV-1 disease progression with introduction to CART, in which CD4+ T cell count and HIV-1 RNA levels are depicted against treatment timeline. CD4+ T cells are rapidly declining, while HIV-1 RNA copies are steadily increasing prior to CART introduction. Once treatment begins, CD4+ T cell count recovers, while measurable HIV-1 RNA levels are at a steady decline. (Adapted from Rohrbach, J., et al.)

HIV-Associated Neurocognitive Disorders

Prior to treatment options which were not introduced into the mid-1990s, HIV-associated dementia (HAD) was relatively common affecting at least 20 percent of HIV-1 infected individuals. HAD is the most severe form of cognitive impairment associated with infection and is described as, “marked cognitive impairment involving at least two cognitive domains that substantially interferes with daily functioning” (23, p. 234). Almost always fatal, HAD has substantially declined since the use of CART and is now rare in the developed world. Still, CART compliant HIV-1 positive individuals experience a spectrum of neurocognitive, behavioral and motor dysfunctions, decreasing their quality of life. Collectively, these infection-

associated inflammatory complications are known as HAND, or HIV-Associated Neurocognitive Disorders, and its neuropathogensis remains an important unresolved issue (1-3, 23). Historically, encephalitis and neuronal loss were thought to play a central role in the pathogenesis of HAD yet these pathologies are no longer typical, therefore no longer sufficient in providing an explanation of the neurological dysfunction in the CART era. The continuation of HAND pathology, despite viral treatment plans, suggest an underlying pathophysiology more likely associated with the functional alterations in neurons (7, 8).

Neurological involvement and changes in brain structure occurs very rapidly after infection; within the first few months following infection, reductions in brain volume, decreases in white matter and increased permeability of the blood-brain barrier have been observed. Moreover, an increase in circulating levels of inflammatory cytokines, acute metabolic disturbances, and immune activation accompany measurable deficits in cognitive and psychomotor functions (7, 8). Unfortunately, many of these modifications do not improve and even have been shown to worsen over time following the initiation of CART, although systemic viral suppression has been achieved.

The relative inaccessibility of the affected brain tissue hinders our understanding of the pathogenic mechanisms underlying HAND; although, contemporary pathological studies of CART-treated individuals report unfavorable changes in white matter integrity, with clear signs of inflammation and neuronal damage (7, 8). This neuronal dysfunction may be due to a number of infected cells such as perivascular macrophages, astrocytes and microglia via a range of mechanisms poorly defined. CART-compliant patients have limited brain-localized HIV-1

replication suggesting that HAND is not the sole consequence of viral replication but may be the result of viral protein expression in infected glial cells which are able to induce toxicity and death of nearby neuronal cells (23, 31). Early and progressive disturbances of bioenergetics, as well as, evidence for abnormal glutamate homeostasis have been implicated in the cause of neuronal injury and death (23). A model proposed by Saylor et al., outline the possible neuropathogenic mechanisms that contribute to HAND:

> HIV-infected macrophages and microglial cells release neurotoxic viral proteins that trigger astrocyte activations, which results in increased glutamate release and reduced glutamate uptake. Elevated extracellular glutamate levels cause neuronal bioenergetic disturbances that lead to aberrant synaptodendritic pruning and neuronal injury. Moreover, systemic inflammation and microbial translocation products lead to microglial activation and increased production of chemokines and cytokines that contribute to neuronal injury (23, p. 240).

Extracellular Vesicles and HIV-Associated Neurocognitive Disorders

To date, the mechanism by which HIV-1 infected monocytes induce neurotoxicity to neighboring cells is unknown, although a number of studies suggest extracellular vesicles may be responsible (12-14, 16, 17, 34). Extracellular vesicles packaged with pathological proteins, such as amyloid beta and alpha-synuclein, have been shown to induce pathology in neighboring neuronal cells of neurodegenerative diseases including Alzheimer's and Parkinson's, respectively (6, 15, 18, 21). Furthermore, there is emerging evidence that HIV-1 infected cells induce the release of extracellular vesicles containing viral RNA, microRNA and viral proteins resulting in the altered gene expression and other pathological consequences in neighboring cells exposed to these extracellular vesicles. This extracellular vesicle-mediated neurotoxicity

may be the source of neuropathology in HAND (12-14, 16, 17, 34). If so, neurotoxic extracellular vesicles may contribute to HAND symptoms in CART treated patients who continue to present a significant reduction or even minimal levels of ongoing viral replication. As such, it is possible that the role of extracellular vesicles in HAND is similar to their role in other, above mentioned, neurodegenerative diseases. There are a number of HIV-1 RNA and proteins that have been implicated in the neuropathological spread HAND, yet this study will focus on three HIV-1 proteins, Nef, Tat and Vpr, which have been implicated in the progression of HAND, and are known to be associated with extracellular vesicles.

Nef, or Negative Regulatory Factor, is a 27-34 kDa myristoylated protein involved in multiple functions during the replication cycle of HIV (22). Nef is known to increase viral infectivity through various actions such as activation of T cell signaling pathways, promoting particle release, causing CD4 receptor down modulation and anti apoptotic signaling (9, 10). This HIV-1 protein consists of a N-terminal myristoyl (14-carbon) lipid attached to the second glycine reside and many positive charges in the first 22 amino acids, constituting Nef as a membrane-associated protein (22).

Nef expression occurs early during HIV-1 infection of CD4+ T cells, macrophages and astrocytes, and has been known to be released form these cells as a cargo protein in extracellular vesicles (9,10). Neurotoxic effects of Nef including neurological degeneration, cytokine production and negative alterations in cellular pathways were discovered using recombinant Nef on human glial cells and neurons. Moreover, animal studies in rats exhibited HIV-1 Nef-induced neurocognitive impairments (89). Lastly, a recent study performed by

Saribas et al., concluded that HIV-1 Nef is released in extracellular vesicles derived from primary human astrocytes and that these vesicles are taken up by primary human neurons, causing axonal and neurite degeneration (88).

The HIV-1 protein Tat, or Trans-Activator of Transcription, consists of 86-101 amino acids depending on the subtype and has been suggested as a causative agent in HAND due to its neuroexcitatory and neurotoxic abilities (11). Being one of the three early encoded proteins, Tat is required for viral replication through its interaction with its response element of the HIV-1 long terminal repeat, allowing for the phosphorylation of RNA polymerase II thus resulting in the synthesis of HIV-RNA transcripts (11). Furthermore, Tat has been shown to be released by HIV-1 infected CD4+ T cells and taken up by uninfected “bystander” T cells directly resulting in cellular apoptosis. It has been hypothesized that due to its lack of signal sequence, Tat may follow an unconventional secretory pathway allowing for its release (90).

Tat is transported across the blood brain barrier by systemic circulation, secreted by infected macrophages and microglia, and has been detected in brain of patients with HAND. Tat has also been associated with extracellular vesicles released from HIV-1 infected CD4+ T cells and when applied to neurons, results such as shorter or no visible neurites and significant neuronal cell death became apparent (90). These results suggest that extracellular vesicle associated Tat is biologically active. Furthermore, a recent study described by Hui et al., concluded that Tat was found to induce significant neuronal cell death from 48 hours of treatment, with a maximum death rate of 50% after 96 hours. After incubation of Tat with neurons, Tat was found to be compartmentalized in endolysosomes; moreover, significant size

increases and aggregation of endolysosomes was observed (90). Interestingly, autophagic dysfunctions have been implicated in the pathogenesis of HAND and Tat treated neurons have been shown to have decreased levels of pro-autophagic proteins, and increased levels of autophagic inhibitory proteins (90).

The Viral Protein R, or Vpr, is a 14 kDa protein which induces G2 cycle arrest and causes apoptosis in proliferating cells (30, 32). In the context of macrophages, Vpr has been known to interact with molecular pathways resulting in the sequestration of proinflammatory transcriptional activators causing immunosuppression, thus allowing for the establishment and maintenance of a systemic infection. Vpr has been identified to modify host cell energy metabolism, proteasome function, and oxidative status, yet while this protein has been extensively studied in the context of HIV-1 infection, the precise mechanism of action remains enigmatic (91).

Recently James et al. described VPR as having a, “unique role in neuropathogensis” and that through extracellular vesicle based intercellular communication VPR has deleterious effects (30, p. 409). Furthermore, VPR was found among the extracellular vesicle population released from HIV-1 infected lymphocytic cells in a study published by Li et al. in 2013 (31).

Extracellular Vesicle Formation

Originally thought to be the cell’s disposal mechanism of discarding unwanted materials, extracellular vesicles have, in the last twenty years, become a topic of interest as they have been implicated in various cellular processes such as cell proliferation, differentiation, death and cellular immune responses (33, 34). A look into the cargo of extracellular vesicles allows for

the presumption that these proteins, nucleic acids, miRNAs, and other cargoes are specifically and intentionally packaged into extracellular vesicles, rather than representing “trash” packaged for the removal from the cell. Extracellular vesicles, ranging in size from 30 to 1000 nm, are often categorized based on size into more precise populations such as exosomes, microvesicles, ectosomes or apoptotic bodies; for the purpose of study I will continue to utilize the inclusive term “extracellular vesicles”.

Extracellular vesicles may be the result of secretion directly from the plasma membrane, released following the endocytic pathway, or can be the product of autophagic unconventional secretion (19, 20, 56-58). The biogenesis of extracellular vesicles released directly from the plasma membrane are the result of outward budding and fission of the plasma membrane. A number of events will allow for their release, such as the redistribution of phospholipids, contraction of actin-myosin machinery or a calcium influx and hypoxia, to name a few (24, 25, 28). A more detailed cascade of events allowing for extracellular release directly from the plasma membrane includes the activation of phospholipase D via ADP-ribosylation factor 6 this, in turn, allows for the recruitment of extracellular signal-regulated kinase (ERK). ERK phosphorylates, thereby activating the myosin light chain kinase, triggering the release of extracellular vesicles (24, 25, 28).

Endosomes are clatherin-coated vesicles located within cells and can be derived either from the exocytic or endocytic pathways (25, 49, 54, 85). Endosomes can be further classified into early, late, or recycling endosomes. Early endosomes are the first to receive incoming cargo and fluid, they have a highly dynamic structure with a high propensity to undergo homotypic

fusion. Early endosomes mature into either the recycling endosome transferring cargo to the plasma membrane, or the late endosome resulting in the enrichment of tetraspanins and often a large accumulation of intraluminal vesicles (ILVs) (25, 49, 54, 85). The formation of ILVs, as well as the protein incorporation into ILVs, is driven by a number of proteins together known as the endosomal sorting complexes required for transport (ESCRT). Upon acquiring multiple ILVs, the late endosome can also be referred to as a multivesicular body (MVB). Often, the late endosome/MVB fuses with the lysosome resulting in degradation; however, a separate fate is fusion with the plasma membrane, giving way to extracellular vesicle release as the late endosome/MVB releases it's ILVs into the extracellular milieu (25, 49, 54, 85).

Extracellular vesicles as a product of autophagic unconventional secretion is a multistep process, involving a number of distinct and dynamic membrane compartments. The exact mechanisms and pathways responsible for autophagic unconventional secretion are unknown, yet is thought to play a role in the secretion of cytosolic cargo of which lack signals of export. Autophagic secretion begins with the process of macroautophagy whereby elongation of a double membrane, or phagophore, is initiated via the ATG1/ULK1 complex (66, 70, 75). While sequestering cytosolic cargos, the phagophore matures into the double-membrane vesicle known as the autophagosome, driven by the lipidation of the LC3 protein. This autophagosome continues in maturation, accumulating a number of ILVs, possibly fusing with other nearby MVBs to form what is known as the amphisome (66, 70, 75). This amphisome can follow one of two fates: fusion with the lysosome in which enclosed cargo meets degradative enzymes such as glycosidases, proteases and sulfatases, or fusion with the plasma membrane resulting in the

release of the amphisome's ILVs as extracellular vesicles (66, 70, 75, 82-84). Interestingly, the idea that the two pathways are underway suggest that different subpopulations of ILVs exist simultaneously within cells, one population destined for degradation, the other released as extracellular vesicles.

Tetraspanins Give Way to Extracellular Vesicle Biogenesis

Tetraspanins belong to a conserved transmembrane family of glycoproteins typically consisting of 200-300 amino acids (28, 29, 45). Often tetraspanins act as scaffolding proteins, anchoring multiple proteins to one area of the plasma membrane in what as known as a cluster of differentiation (CD); CDs have been shown to be a successful tool for in the immunophenotyping of a variety of cell types, as well as extracellular vesicles. Kowal et al., propose the differential separation of extracellular vesicles via immuno-isolation using CD9, CD63 and CD81 in hopes of allowing a, "proper evaluation of the molecular mechanisms of biogenesis and secretion and the respective functions of subtypes of extracellular vesicles" (28, p. 969).

Ranging from 25-65 kDa, due to post-translational glycosylation, CD63 was the first characterized tetraspanin (45). This ubiquitously expressed protein is localized within the endosomal system and the cell surface. Most often associated with the late endosome/MVB and lysosome, CD63 consists of a particular consensus motif required for endocytosis at the plasma membrane and has also been implicated in direct lysosomal targeting (45). CD63 is approximately seven times as enriched in the ILVs of the MVB, when compare to the

endosomal limiting membrane. Interestingly, incorporation of CD63 into the ILVs seems to be independent of the ESCRT machinery (45).

CD9 is a 24 kDa tetraspanin and is reported to exhibit both promigratory and antimigratory properties via integrin-dependent signaling (29). Associated with the plasma membrane, CD9 has been implicated in muscle cell fusion, as well as egg-sperm fusion. Interestingly, CD9 is often associated or in complex with CD81, a 26 kDa cell surface tetraspanin; their association has been implicated in tumor cell behaviors such as motility via ligand attachments and breast cancer cell morphology (29). Alone, CD81 plays a significant role in cell attachment/entry of Hepatitis C, the pathogenesis of the *Plasmodium* species, as well as the virion assembly and release of HIV-1 (28, 29).

CHAPTER TWO

NOVEL APPROACHES TO ANALYZING SINGLE EXTRACELLULAR VESICLES

Rather than assuming homogeneity within the extracellular vesicle population, we hypothesize that distinct populations of extracellular vesicles are released, and that environmental conditions can alter this population. Previous work in the field has examined these extracellular vesicles in bulk, examining western blots of cellular protein or RNA levels present in all collected extracellular vesicles via RT-PCR, from a given cell population. To determine the heterogeneity of the populations, I aim to evaluate the populations of secreted extracellular vesicles at the single vesicle level. By creating new methodologies for studying single extracellular vesicles, this allows for a more thorough understanding of their suspected involvement in a variety of pathologies such as HAND.

In order to concentrate the extracellular vesicle population differential centrifugation was utilized in this study, although there are various methods of extracellular vesicle purification including immunomagnetic isolation methods, ultrafiltration methods, or sucrose gradient fractionation methods. Yet, as each method has its challenges we have decided to employ the the “gold standard” of purification methods, of which is the most common among vesicle research to date (92).

Using techniques successful in studying virions, I have similarly incorporated fluorescent markers into secreted extracellular vesicles by fusing a fluorophore such as GFP, to the first 15

amino acids of the Src protein (S15); this provides the foundation of plasma membrane incorporation due to the particular positive charge and propensity to undergo a myristoylation reaction. The first 15 amino acids of the Src protein undergo a myristoylation reaction at the second Glycine reside from the N-terminal, acting as a plasma membrane anchor. Furthermore, with its high number of arginines and lysines, this particular stretch of basic amino acids increases Src's propensity for the plasma membrane. This S15 membrane marker has been shown to incorporate throughout the plasma membrane, fluorescently tag budding virions from the plasma membrane and now has been successful in providing a fluorescent marker of secreted extracellular vesicles. Following cellular expression of the S15 construct, released extracellular vesicles can be analyzed through protein co-localization analysis with the utilization of the canonical vesicle markers CD9, CD63 and CD81, as well as lysosomal marker LAMP1 and TSG101. Quantification via wide-field deconvolution microscopy combined with imaging software, allows for the analysis of extracellular vesicles at a single vesicle level.

Because of its uniformity and sensitivity, wide field deconvolution microscopy is an ideal tool to quantify the fluorescent intensity of extracellular vesicle populations. For an unbiased, high throughput analysis algorithms are generated utilizing Bitplane Imaris imaging software to create three dimensional surfaces around individual extracellular vesicles (Figure 3). For example, surfaces are created around the S15-GFP membrane marker and the fluorescence intensity of other, co-localized markers such as the tetraspanin CD63 or LAMP1 within these individual S15 surfaces, are exported as individual events for analysis. In this way, it is possible

to analyze and compare large quantities of extracellular vesicles containing the S15-GFP and Immunofluorescent markers to determine their heterogeneous nature.

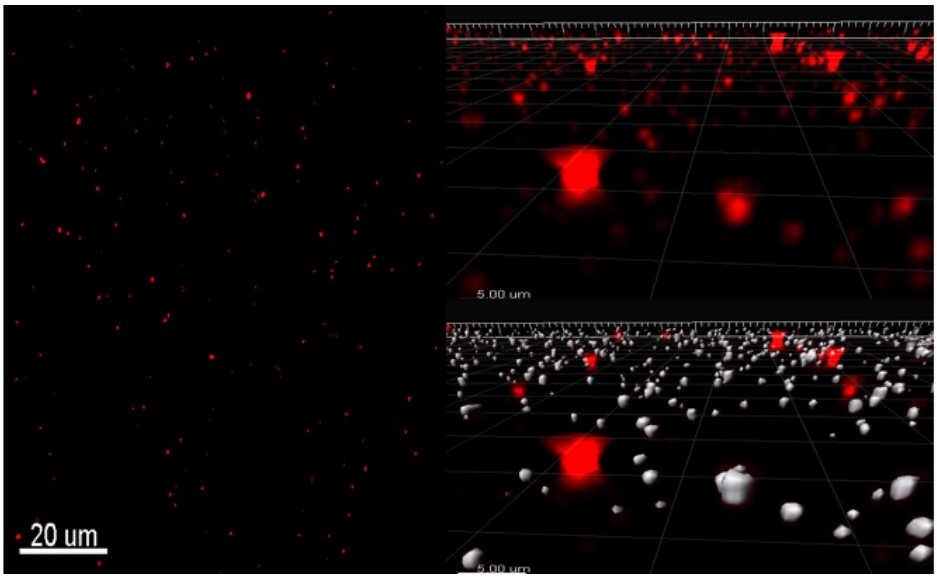

Figure 3. Representative Sample of Surface Masks. The left panel shows an example of an acquired image in one fluorescent channel of interest. Surface algorithms are generated to detect puncta within various parameters.

CHAPTER THREE

OVERALL HYPOTHESIS AND EXPERIMENTAL GOALS

The pathways of extracellular vesicle communication and their selective cargoes can become hijacked in the context of many diseases, including viral infection, thus contributing to the pathogenesis of HAND. In HIV-1 positive patients undergoing CART, viremia is potently suppressed, preventing the development of AIDS. However, these CART-suppressed individuals still exhibit non-AIDS disease states such as HAND, which include neurological disorders with varying severity. Current literature suggests that extracellular vesicles may be involved in the pathogenesis of HAND in the CNS as they are believed to be transferring HIV-1 proteins, including Tat, Nef and Vpr, to nearby neuronal cells. Overall, I hypothesize that extracellular vesicles containing HIV-1 proteins are of a heterogeneous population. By achieving a better understanding of the molecular and cellular mechanisms which lead to the pathology of HAND in HIV-1 patients, therapeutic interventions can become a possibility.

To begin addressing the pathogenesis of HAND in the CNS, a foundation of study must be established and primitive questions must first be addressed. Ultimately analyzing extracellular vesicles derived from HIV-1 infected cells is most applicable in a disease-state model, yet to analyze the population of extracellular vesicles released following HIV-1 infection

would require a reliable method of separating virus from extracellular vesicles. Physical and chemical characteristics, as well as biogenesis pathways are almost identical between extracellular vesicles and virions causing an analysis such as this very challenging. In a foundational study such as this the main focus is to validate a method of single vesicle analysis, as well as just begin the study of vesicle populations containing HIV-1 proteins.

Through the achievement of two experimental goals, I hope to better understand populations of extracellular vesicles containing HIV-1 proteins and approach the answers to some of the following questions. Do extracellular vesicles contain HIV-1 proteins Tat, Nef or Vpr? Are these vesicles similar to one another? Can we decipher the possible biogenesis of subsets of extracellular vesicle populations? Will the canonical biomarkers CD9, CD63 and CD81provide useful information of these extracellular vesicles? Will LAMP1 or TSG101 allow us to draw conclusions of their biogenesis?

Experimental Goal: Determine if distinct populations of extracellular vesicles are released within and among cell types. Through the developed method previously described in Chapter Two, I aim to analyze extracellular vesicle populations at the single vesicle level. The common vesicle markers CD9, CD81 and CD63, as well as LAMP1 and TSG101, will be utilized to characterize populations based on their co-localization analyses. Assessment at the level of a single vesicle will shed light on their heterogeneity and begin unique analysis of their suspected involvement in a variety cellular processes.

Experimental Goal: Define the cell surface markers of extracellular vesicles containing HIV-1 proteins relevant to HAND. Following the validation of single extracellular vesicle analysis,

I aim to determine if/how HIV-1 viral protein expression, specifically Tat, Nef or Vpr, influences the quantity and quality of extracellular vesicle populations. Again, the common vesicle markers CD9, CD81 and CD63, as well as LAMP1 and TSG101, will be utilized to characterize these populations of particular interest. Simultaneous assessment of these markers on thousands of extracellular vesicles will allow a previously unachieved appreciation for the specific vesicle populations produced before and after HIV-1 viral protein expression.

CHAPTER FOUR

DISTINCT POPULATIONS OF EXTRACELLULAR VESICLES ARE RELEASED WITHIN AND AMONG CELL TYPES

Materials and Methods

Cell Culture.

HEK 293T (293T) cells were cultured at 37 degrees Celsius and 5 percent Carbon Dioxide in Dulbecco's modified Eagle's Medium (DMEM) containing phenol red (Invitrogen), supplemented with the addition of 10 percent fetal bovine serum (FBS) (Hyclone), 100 IU/ml penicillin, 100 ug/ml streptomycin and 10 ug/ml ciprofloxacin hydrochloride.

Mesenchymal Stem Cells (MSCs) were cultured at 37 degrees Celsius and 5 percent Carbon Dioxide in Iscvoe's Modified Dulbecco Minimum Essential Medium (IDMEM) containing phenol red (Invitrogen), supplemented with the addition of 10 percent fetal bovine serum (FBS) (Hyclone), 10 percent horse serum (Hyclone), 100 IU/ml penicillin, 100 ug/ml streptomycin and 10 ug/ml ciprofloxacin hydrochloride.

Transfection of S15 GFP Construct and Extracellular Vesicle Collection.

293T cells were transfected at approximately 60 percent confluency using Polyethylenimine (PEI), with equal parts of psPax2 and S15-GFP plasmids. Cell supernatant was collected 48, 72 and 96 hours post-transfection for extracellular vesicle collection via differential ultracentrifugation. For the vesicle collection, collected supernatant was first spun

at 4,000g for 20 minutes, 10,000g for 30 minutes and 100,000g for 70 minutes. The pelleted vesicles were then re-suspended in PBS and spun at 100,000g for 70 minutes. All differential centrifugation was performed in 4 degrees Celsius. Concentrated extracellular vesicle pellets were re-suspended in PBS and stored at -80 Celsius.

Immunofluorescent Staining.

For extracellular vesicle visualization experiments, collected vesicles were spinoculated onto glass coverslips at 13 degrees Celsius for 2 hours at 1200g and subsequently fixed with a solution consisting of 0.1 M PIPES and 3.7 percent formaldehyde (Polysciences) for 5 minutes. Following fixation, vesicles were incubated with the following possible primary antibodies at a concentration of 1:1000: mouse anti-CD9 (BD Pharmigen), mouse anti-CD63 (BD Pharmigen), mouse anti-CD81 (BD Pharmigen), or mouse anti-TSG101 (Santa Cruz Biotechnology Inc.) along with the rabbit anti-Lamp1 antibody (Abcam), in a PBS block solution supplemented with 10 percent normal donkey serum (NDS), and 0.01 percent NaN3 for 1 hour. Following primary antibody incubation vesicles were incubated with their respective secondary antibody conjugated to a fluorophore, either donkey anti-mouse 594-conjugated or donkey anti-rabbit 647-conjugated, at a concentration of 1:400, for 20 minutes in the same, above described PBS block solution.

Wide-Field Deconvolution Microscopy and Analysis.

Extracellular vesicle images were taken on a DeltaVision wide field fluorescent microscope (Applied Precision, GE) outfitted with a digital camera (CoolSNAP HQ;

Photometrics), while using a 1.4 numerical aperture, and 60 X objective lens. The acquired images were deconvolved with the SoftWoRx deconvolution software (Applied Precision) and analyzed on Bitplane: Imaris software version 7.6.4.

Puncta were analyzed for vesicle-like characteristics, such as size and sphericity, and a surface algorithm was built around the S15-GFP signal. The maximum fluorescence intensity found within these puncta was then analyzed and cross analyzed with the other perspective channels. Finally, all acquired images were subjected to the same algorithm via the Batch Coordinator tool (Bitplane) to each respective signal. All statistical analyses and graphs were created using GraphPad Prism version 5.00 or 6.00 (GraphPad Software, Inc.).

Results and Conclusions

To validate the proposed methodology of single vesicle analysis, extracellular vesicles derived from transfected S15-GFP 293T cells were analyzed following collection, immunofluorescent staining, and wide-field deconvolution microscopy. Results following the CD63/LAMP1 protein co-localization analysis reveal the vesicle population as heterogeneous; whereby, only 4.2 percent of S15-GFP positive puncta are also positive for CD63 and LAMP1. Furthermore, S15-GFP 293T vesicles are more likely to be CD63 positive, rather than LAMP1 positive, as CD63 positive puncta account for 41.5 percent, as opposed to the 1.0 percent found to be positive for LAMP1. Interestingly, a large proportion of S15 positive 293T extracellular vesicles, 53.3 percent, are negative for both LAMP1 and CD63.

S15-GFP 293T extracellular vesicle co-localization analysis with surface markers CD81 and LAMP1 reveal similar results in that a small percentage, 3.5 percent, are LAMP1 positive. This population of extracellular vesicles are more likely to be CD81 positive, revealing a 51.2 percent positive expression profile, and 12.3 percent positive for both LAMP1 and CD81. Similarly, this analysis reveals a significant proportion of S15-GFP extracellular vesicles are negative for either CD81 or LAMP1, 33.0 percent.

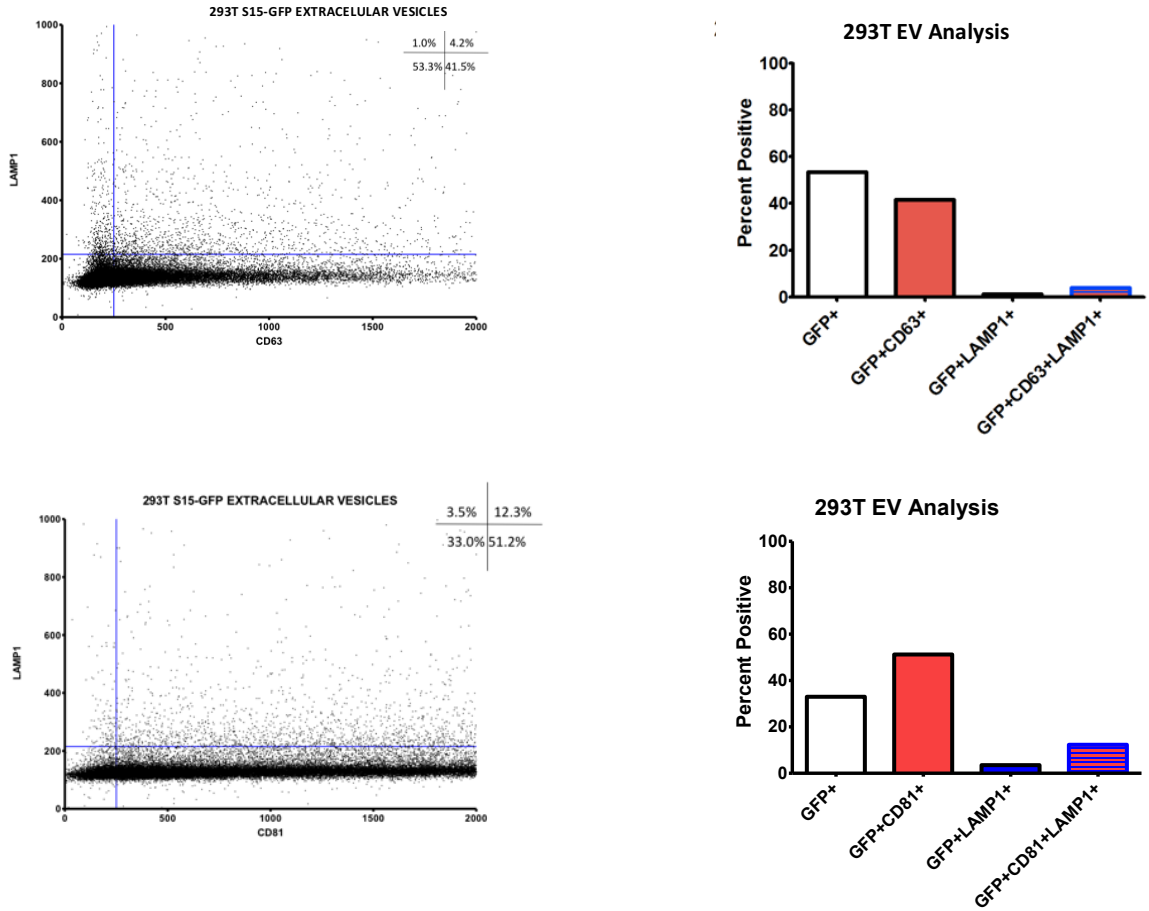

Figure 4. 293T Extracellular Vesicle Analysis. Here, we are depicting the colocation of the S15-GFP surface marker with either LAMP1 and CD63, or LAMP1 and CD81. Dot plots are sectioned into quadrants with corresponding percentages. The upper right quadrant quantifies the triple positive puncta, whereas the lower left quadrant quantifies the S15-GFP positive puncta alone. Bar graphs represent the summation of each quadrant, accounting for 100 percent of the S15-GFP positive puncta.

Following analysis of S15-293T extracellular vesicles and determining that the methodology utilized for individual vesicle analysis has been successful, it was of interest to examine another cell type to determine if the vesicle populations are distinct from one another. Extracellular vesicles derived from GFP MSCs were analyzed for their protein co-localization, with the same canonical markers utilized in characterizing S15-GFP 293T extracellular vesicles.

Interestingly, the protein profile derived from GFP MSC extracellular vesicles was very unique, in comparison to the S15-GFP 293T derived vesicles. Extracellular vesicles derived from GFP MSCs had a high propensity for LAMP1, and showed much lower levels of the tetraspanin protein markers CD63 and CD81. Again, this analysis reveals a significant proportion of GFP MSC extracellular vesicles are negative for either CD81 or LAMP1, 30.5 percent, and negative for either CD61 or LAMP1, 51.2 percent.

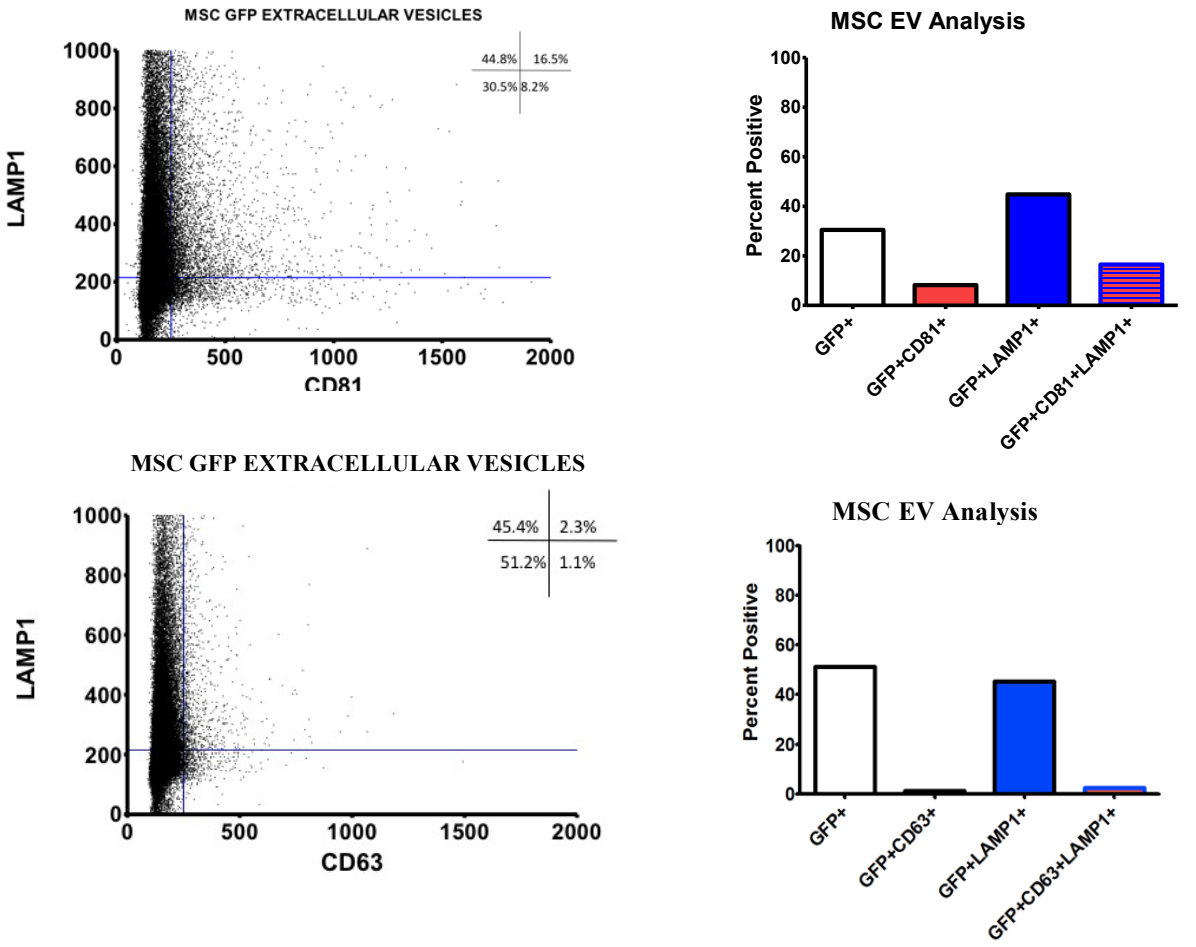

Figure 5. MSC Extracellular Vesicle Analysis. Here we are depicting the colocalization of the MSC GFP surface marker with either CD81 and LAMP1, or CD63 and LAMP1. Dot plots and bar graphs are arranged in the same manner as described in Figure 4.

Overall, when comparing the vesicle populations of S15-GFP 293T and GFP MSCs, it is apparent that 293T extracellular vesicles have a much higher overall intensity level than the MSCs in GFP expression, CD63 and CD81 tetraspanin expression. Interestingly, intensity of LAMP1 differ in that the MSC extracellular vesicles have a much higher expression profile, than their 293T counterpart. Figure 6 depicts the comparison analysis of max intensity of each individual puncta, analyzed from within their own channel surface mask. Worth observing is the

puncta count from each channel surface mask; not always are the most intense puncta the most populous.

Although, it must be addressed that the conjugate antibody of tetraspanins CD63 and CD81 are from mouse; therefore, these data must be taken lightly as MSCs are derived from mice. Fortunately, the LAMP1 conjugate antibody is against rabbit allowing the data to be fully interpreted as presented.

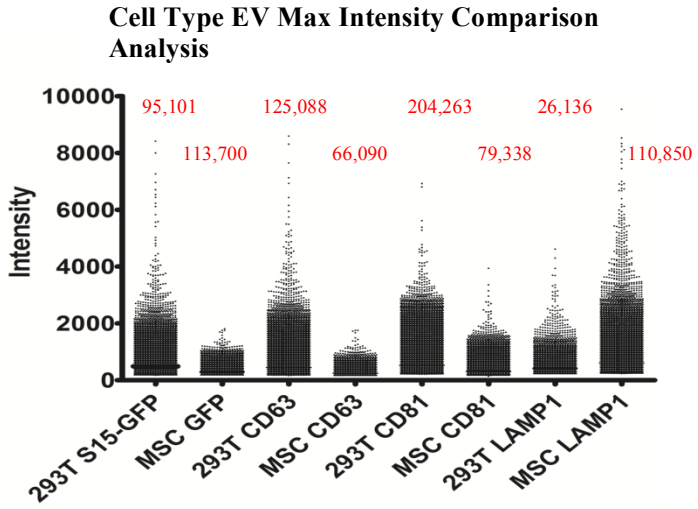

Figure 6. Cell Type EV Max Intensity Comparison
Here, we are comparing the fluorophore signal intensity of all puncta from each surface mask created. The red numbers represent the total puncta number.

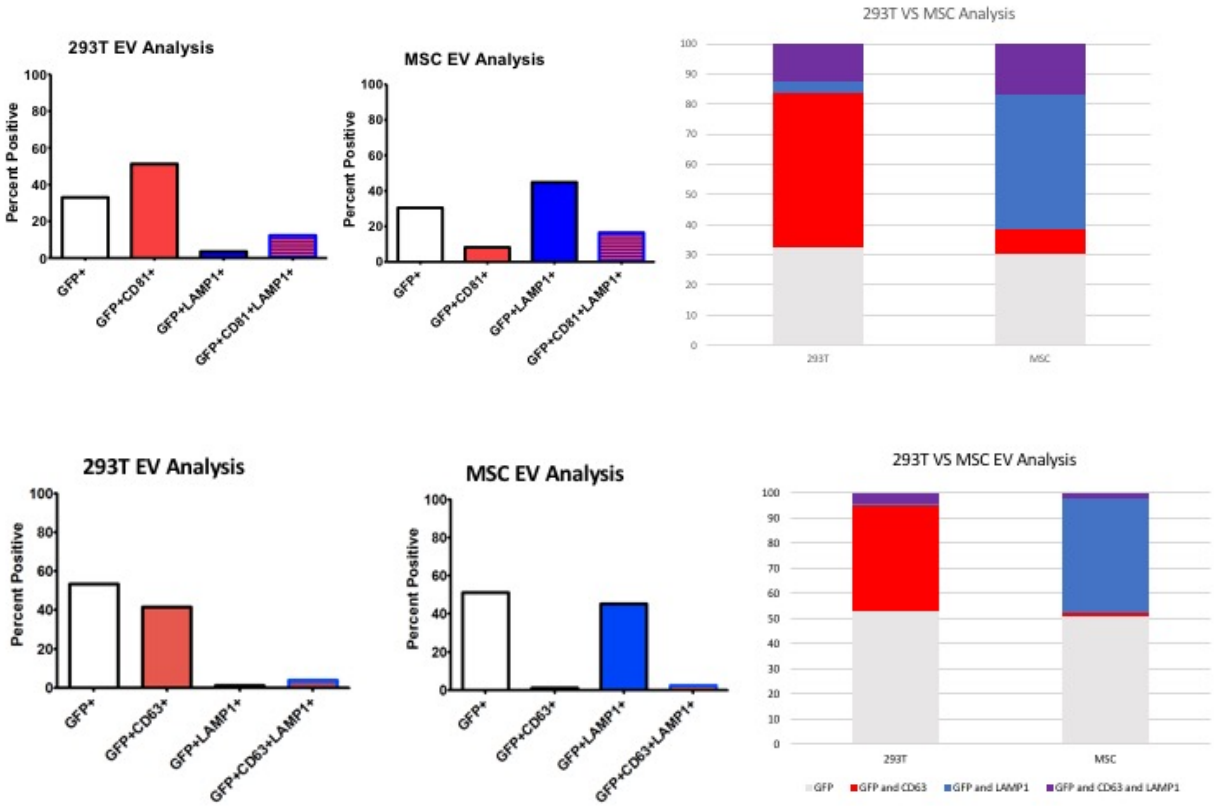

Figure 7: Extracellular Vesicle Protein Co-Localization Analysis. This data shows the summation of both S15-GFP 293T and GFP MSC vesicle co-localization analyses with either CD81, LAMP1, CD81 and LAMP1 (top), or CD63, LAMP1, or CD63 and LAMP1 (bottom). Bar graphs represent the summation of each protein co-localization analysis, with corresponding colors.

CHAPTER FIVE

CELL SURFACE MARKERS OF EXTRACELLULAR VESICLES CONTAINING HIV-1 PROTEINS RELEVANT TO HAND

Materials and Methods

Cell Culture.

HEK 293T (293T) cells were cultured at 37 degrees Celsius and 5 percent Carbon Dioxide in Dulbecco's modified Eagle's Medium (DMEM) containing phenol red (Invitrogen), supplemented with the addition of 10 percent fetal bovine serum (FBS) (Hyclone), 100 IU/ml penicillin, 100 ug/ml streptomycin and 10 ug/ml ciprofloxacin hydrochloride.

THP-1 cells were cultured at 37 degrees Celsius and 5 percent Carbon Dioxide in Roswell Park Memorial Institute medium (RPMI) containing phenol red (Invitrogen), supplemented with the addition of 10 percent fetal bovine serum (FBS) (Hyclone), 100 IU/ml penicillin, 100 ug/ml streptomycin and 10 ug/ml ciprofloxacin hydrochloride.

Protein-GFP Fusion Constructs.

Expression plasmids encoding HIV-1 proteins Nef, Tat and Vpr were generated by PCR–based strategy. First, HIV-1 viral proteins Tat and Nef were fused to the N-terminus of GFP in a pEGFP-N1 backbone (Figure 7B, 7C). Following this, the Tat-GFP fused protein was subcloned into the multiple cloning site of the lentiviral backbone (pLVX) by PCR-based strategy (Figure 7A).

Transfection of Protein-GFP Constructs and Generation of Stable TAT-GFP Cell Line.

293T cells were transfected at approximately 60 percent confluency using Polyethylenimine (PEI), with either the NEF-GFP-N1, TAT-GFP-N1 or GFP-VPR plasmid. Cell supernatant was collected 48, 72 and 96 hours post-transfection for extracellular vesicle collection via differential ultracentrifugation.

Lentivirus for transduction was produced by transfection of 293T cells with equal parts of vesicular stomatitis virus glycoprotein (VSV-G), packaging construct psPax2, and Tat-GFP-pLVX. Viruses were harvested 48 hours post-transfection, filtered through a 0.45-μm filter (Millipore), and used to transduce THP-1 cells. Cells were selected 48 hours post-transduction in RPMI containing 5 μg/ml puromycin (Sigma-Aldrich).

Extracellular Vesicle Collection.

Collected supernatant was first spun at 4,000g for 20 minutes, 10,000g for 30 minutes and 100,000g for 70 minutes. The pelleted vesicles were then re-suspended in PBS and spun at 100,000g for 70 minutes. All differential centrifugation was performed in 4 degrees Celsius. Concentrated extracellular vesicle pellets were re-suspended in PBS and stored at -80 Celsius.

Immunofluorescent Staining.

For extracellular vesicle visualization experiments, collected vesicles were spinoculated onto glass coverslips at 13 degrees Celsius for 2 hours at 1200g and subsequently fixed with a solution consisting of 0.1 M PIPES and 3.7 percent formaldehyde (Polysciences) for 5 minutes. Following fixation, vesicles were incubated with the following possible primary antibodies at a

concentration of 1:1000: mouse anti-CD9 (BD Pharmigen), mouse anti-CD63 (BD Pharmigen), mouse anti-CD81 (BD Pharmigen), or mouse anti-TSG101 (Santa Cruz Biotechnology Inc.) along with the rabbit anti-Lamp1 antibody (Abcam), in a PBS block solution supplemented with 10 percent normal donkey serum (NDS), and 0.01 percent NaN3 for 1 hour. Following primary antibody incubation vesicles were incubated with their respective secondary antibody conjugated to a fluorophore, either donkey anti-mouse 594-conjugated or donkey anti-rabbit 647-conjugated, at a concentration of 1:400, for 20 minutes in the same, above described PBS block solution.

Wide-Field Deconvolution Microscopy and Analysis.

Extracellular vesicle images were taken on a DeltaVision wide field fluorescent microscope (Applied Precision, GE) outfitted with a digital camera (CoolSNAP HQ; Photometrics), while using a 1.4 numerical aperture, and 60 X objective lens. The acquired images were deconvolved with the SoftWoRx deconvolution software (Applied Precision) and analyzed on Bitplane: Imaris software version 7.6.4.

Puncta were analyzed for vesicle-like characteristics, such as size and sphericity, and a surface algorithm was built around the GFP signal. The maximum fluorescence intensity found within these puncta was then analyzed and cross analyzed with the other perspective channels.

Finally, all acquired images were subjected to the same algorithm via the Batch Coordinator tool (Bitplane) to each respective signal. All statistical analyses and graphs were created using GraphPad Prism version 5.00 or 6.00 (GraphPad Software, Inc.).

Results and Conclusions

Extracellular vesicles may be the result of secretion directly from the plasma membrane, released following the endocytic pathway, or can be the product of autophagic unconventional secretion (19, 20, 56-58). Nef extracellular vesicles are less than 5 percent LAMP1 positive leading us to believe that Nef may be secreted directly from the plasma membrane, as LAMP1 is associated with autophagic unconventional secretion. These data correlate well with the structural model of Nef, as this protein consists of an N-terminal myristoylation, causing Nef to be a membrane-associated protein (Figure 9C). Furthermore, the previously described S15-GFP membrane marker, consisting of a myristoylated glycine residue and positive charges, reveal a similar co-localization analysis with LAMP1 at approximately 5 percent. Lastly, the extracellular vesicles of Nef colocalize more so with the tetraspanins CD63 and CD81, of which are known to be located in the plasma membrane of cells, rather than the late endosome/MVB tetraspanin CD9.

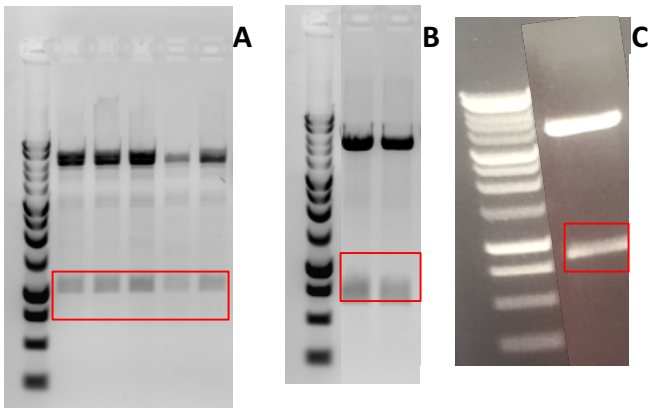

Figure 8. Agarose Gel Electrophoresis of Generated HIV-1 Protein Plasmids. Panel A depicts the Tat-GFP-pLVX clone. Panel B depicts the Tat-pEGFP-N1 clone. Panel C depicts the Nef-pEGFP-N1 clone.

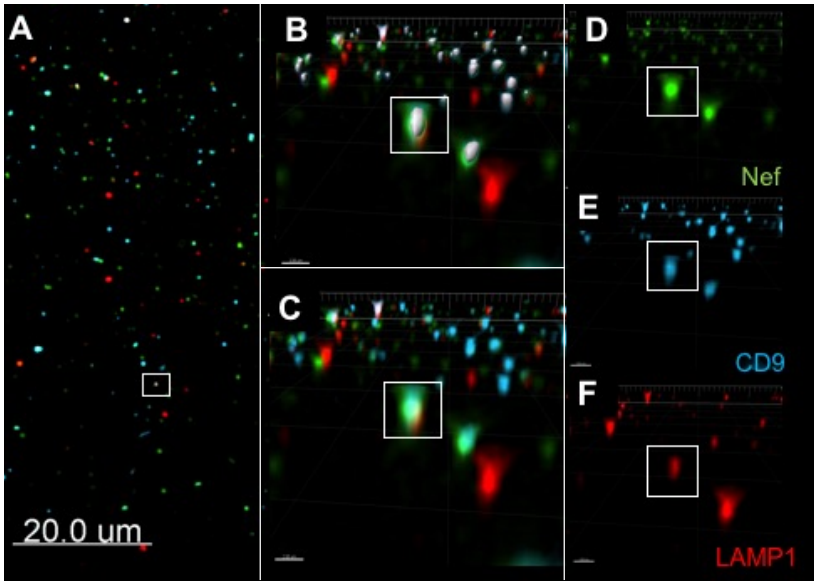

Figure 9. Representative Example of Triple Co-Localization. Panel A is a portion of the total image achieved of which three distinct channels are visible. Panel B reveals a number of surfaces which have been created to detect puncta within the parameters of the set algorithm. Triple colocalization can be detected in panel C, from each individual fluorescent channel: NEF-GFP (D), CD9 (E) and LAMP1(F).

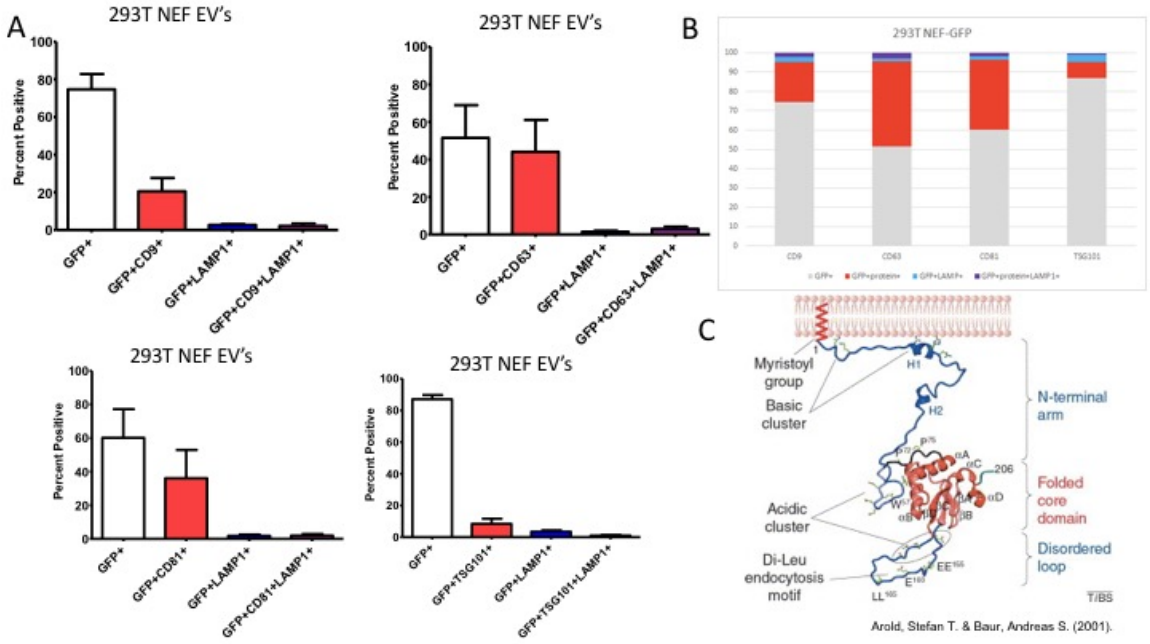

Figure 10. 293T Nef-GFP Extracellular Vesicle Protein Co-Localization Analyses and Protein Structure. (A) This data shows the summation of each Nef-GFP antibody stain; each protein co-localization analysis has 3 total data replicates. Error bars show the standard error of the mean. (B) Bar graphs to represent the summation of each protein co-localization analysis. (C) Structural example of HIV-1 protein Nef.

Unlike Nef extracellular vesicles, Tat profiles are nearing 20 percent positive for LAMP1, suggesting their release is more associated with the autophagic unconventional secretion pathway. Yet, as the data present Tat often colocalizes with CD63 and CD81 as well suggesting their release directly from the plasma membrane. Although confounding, these Tat single vesicle analyses may lead to the conclusion that this particular HIV-1 protein is packaged and released within vesicles from multiple, or more than one pathway.

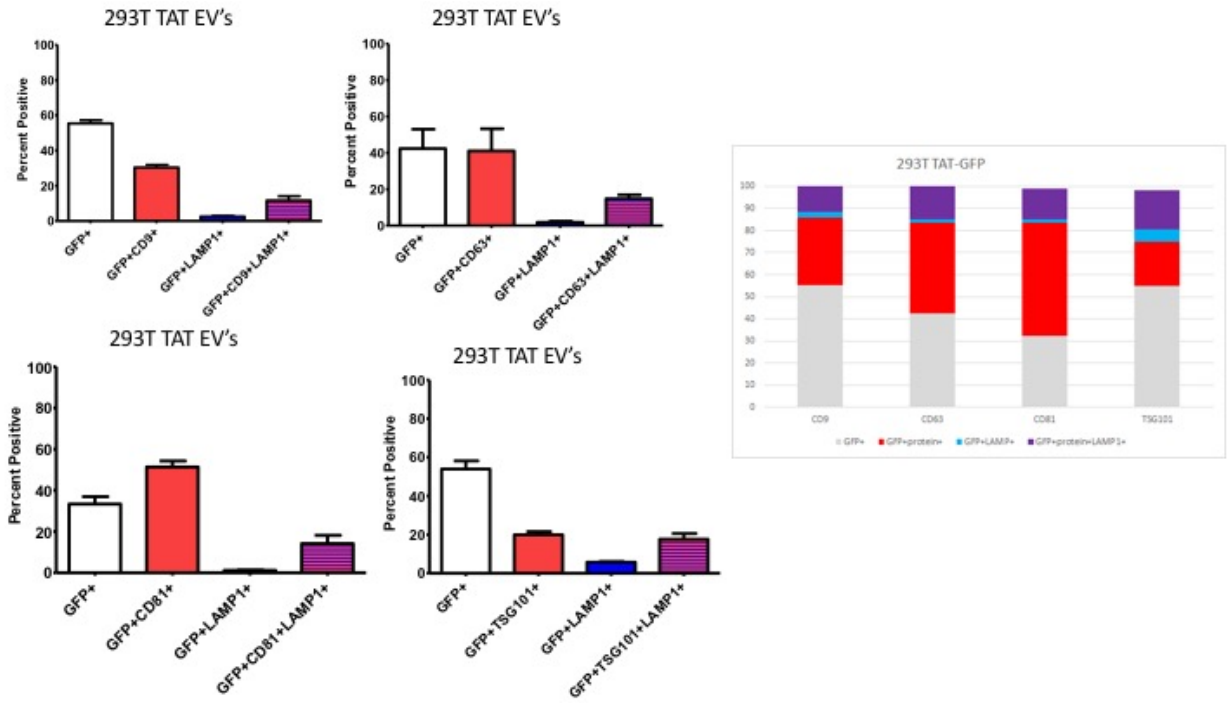

Figure 11. 293T Tat-GFP Extracellular Vesicle Protein Co-Localization. This data shows the summation of each Tat-GFP antibody stain; each protein co-localization analysis has 3 total data replicates. Error bars show the standard error of the mean. Bar graphs to represent the summation of each protein co-localization analysis.

Similar to extracellular vesicles released from Tat-GFP 293T cells, Tat-GFP THP-1 extracellular vesicles are nearing 20 percent positive for LAMP1, yet expression of tetraspanins CD9, CD63, CD81 and ESCRT protein TSG101 have all decreased. Possibly THP-1 Tat vesicles are associated with the autophagic unconventional secretion pathway.

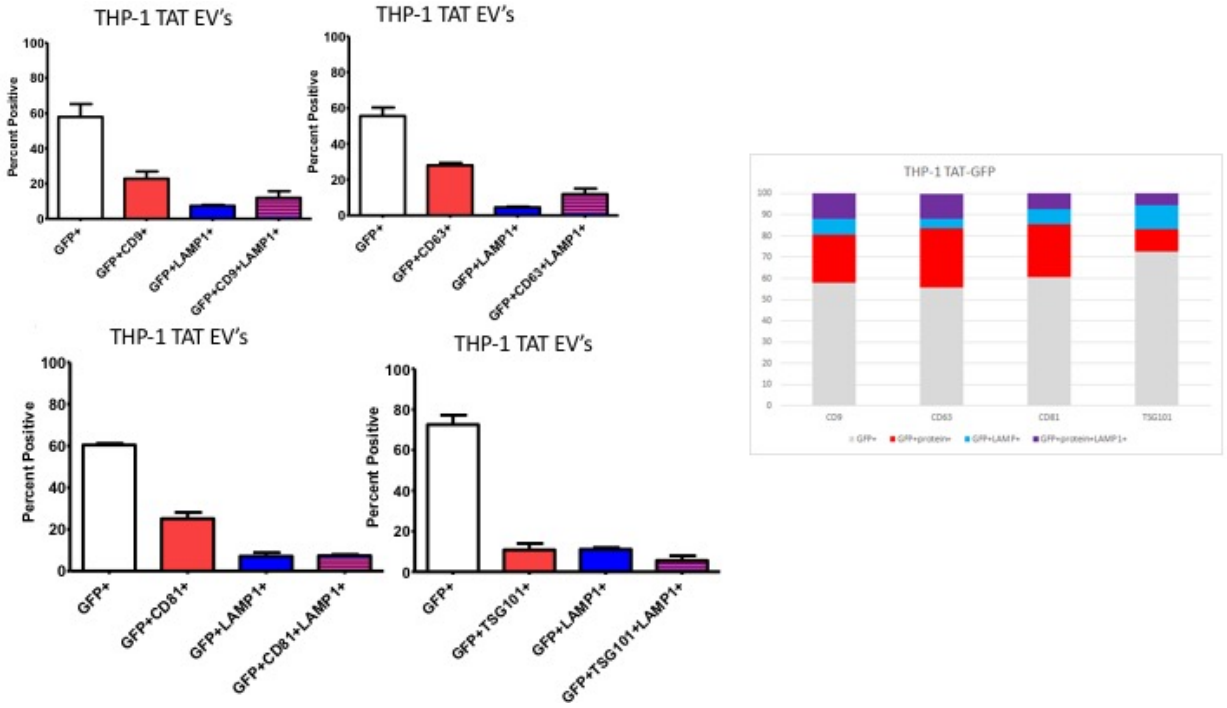

Figure 12. THP-1 Tat-GFP Extracellular Vesicle Protein Co-Localization. This data shows the summation of each Tat-GFP antibody stain; each protein co-localization analysis has 3 total data replicates. Error bars show the standard error of the mean. Bar graphs to represent the summation of each protein co-localization analysis.

Extracellular vesicles released from GFP-Vpr expressing 293T cells present with a protein co-localization profile more similar to 293T Tat-GFP vesicles, than 293T Nef-GFP vesicles. As the data present, Vpr vesicles are nearing 25 percent positive for LAMP1, suggesting their release are more associated with the autophagic unconventional secretion pathway. Of the three HIV-1 protein expressing extracellular vesicle populations, Vpr vesicles have the lowest co-localization with the tetraspanins CD9, CD63 and CD81, yet the highest expression of ESCRT protein TSG101, suggesting that Vpr vesicles may be derived from an unconventional secretion pathway as TSG101 is a protein found within late endosomes/MVB.

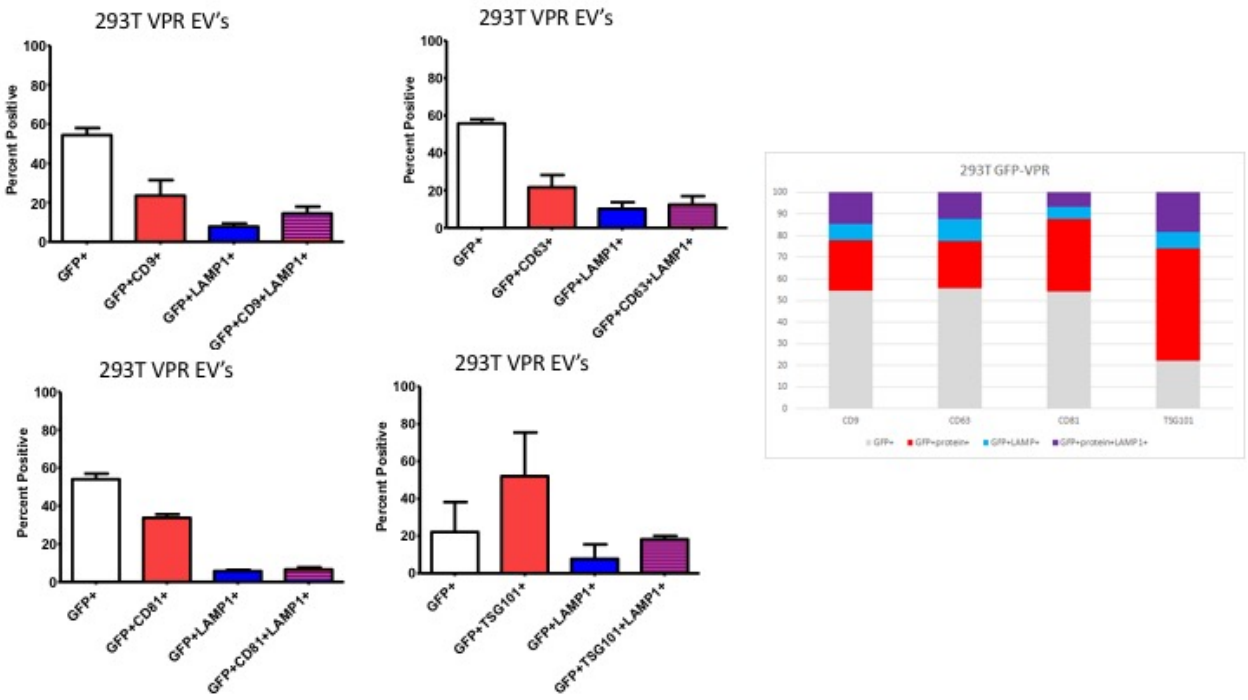

Figure 13. 293T GFP-Vpr Extracellular Vesicle Protein Co-Localization. This data shows the summation of each GFP-Vpr antibody stain; each protein co-localization analysis has 3 total data replicates. Error bars show the standard error of the mean. Bar graphs to represent the summation of each protein co-localization analysis.

CHAPTER SIX

DISCUSSION

Extracellular vesicle analysis at the level of individual vesicles provides a newfound appreciation of their heterogeneous population, allowing for further analysis of possible subpopulations. Prior to this work the techniques most often utilized to study extracellular vesicles were based on the entire population, via western blot or RT-PCR, constraining viewpoints of homogeneity. The validated methodology provided in this study has the potential to be utilized in the examination of various extracellular vesicles released from any set of cells, under a variety of treatment options, allowing a broader understanding of extracellular vesicles. Moreover, through the use of various protein markers such as tetraspanins CD9, CD63 and CD81, as well as ESCRT protein TSG101 and lysosomal marker LAMP1, it may be possible to determine the biogenesis of extracellular vesicles implicated in HAND pathogenesis. Immunofluorescent staining and wide-field deconvolution microscopy coupled with canonical vesicle markers allows for the analysis of subpopulations of extracellular vesicles released into the extracellular milieu.

Results from this study revealed that distinct vesicles are released within and among cell types. The S15-GFP membrane-associated marker was the way in which extracellular vesicles were visualized for further analysis. It was found that S15-GFP 293T vesicles were less than 5 percent LAMP1 positive and were significantly more positive for tetraspanins CD63 or CD81

suggesting their release to be generated directly from the plasma membrane or the classic, exocytic pathway of extracellular biogenesis rather than an unconventional autophagic secretion. This data correlates well with the membrane-association of the S15-GFP marker, yet through our analyses it became apparent that not all extracellular vesicles were S15-GFP positive (especially those that were LAMP1 positive) leading us to believe that it would be beneficial to study extracellular vesicle populations with a more inclusive marker. Possibly membrane-intercalating fluorescent dyes would be a more appropriate tool in the analysis of entire extracellular populations.

This methodology of single vesicle analysis was then applied to a second cell type, MSCs as they were readily available. GFP MSC extracellular vesicles had a unique protein co-localization profile, being much more LAMP1 positive compared to the S15-GFP extracellular vesicles released from 293T cells. Interestingly, MSCs have been shown to have extremely high autophagosome concentration even during basal state which correlates with the data presented here (19). Their profile of tetraspanins CD63 and CD81, are insignificant among the vesicle population, yet as stated previously this may be due, in part, to the fact that the primary antibody for these tetraspanins were against mouse of which MSCs are derived. It would be of interest to analyze MSC extracellular vesicles with the appropriate species type antibodies to determine their true tetraspanin profile.

The extracellular vesicle analyses containing HIV-1 proteins relevant to HAND display the possibility of utilizing this technique of extracellular vesicle analysis within vesicle populations implicated in pathogenesis. HIV-1 proteins Tat, Nef and Vpr were of interest due to

their broad association in HAND, as well as their incorporation into extracellular vesicle populations. The majority of these studies were carried out with the utilization of 293T cells, allowing for the foundation of single vesicle analysis with the incorporation of HIV-1 proteins. As might be expected it would be of great interest to continue such analyses in more relevant cell types, such as THP-1 cells differentiated into macrophages; these cells would bring us one step closer to the CNS resident microglia.

Extracellular vesicles derived from cells over-expressing GFP fusions to each of these proteins of interest, present with unique protein co-localization analyses. The population of Nef-GFP extracellular vesicles was found to be highly associated with tetraspanins CD63 and CD81 and less so with CD9, TSG101 and LAMP1. These data fall in line with the structure of Nef, as myristoylation allows for plasma membrane association, much like the S15-GFP membrane marker. It would be of great interest to determine if other, more HIV-1 applicable cell lines such as THP-1 cells, have similar extracellular vesicle characterizations. Unfortunately for this study time did not permit those analyses.

In comparison, Tat-GFP vesicles, both derived from 293T and THP-1 cells, are more inclined to be positive for all markers including tetraspanins CD9, CD63 and CD81, TSG101, and LAMP1. Quite possibly Tat protein is released within multiple vesicle populations, derived from various biogenesis pathways, as literature suggests states of disease and alterations of cellular metabolism perturb the cells natural extracellular vesicle biogenesis pathways (6, 15, 18, 21). Tat, a protein known to be often secreted from HIV-1 infected cells, may incorporate itself into many extracellular populations for means of exiting the cell.

Lastly, GFP-Vpr extracellular vesicles present with the highest expression of ESCRT protein TSG101; this suggests that their release may be more connected to the classic, exocytic pathway of extracellular biogenesis as TSG101, an ESCRT protein, is often found within late endosomes/MVB. With hopes of studying this viral protein in a more relevant HIV-1 disease model cell line, THP-1 cells were generated to express GFP-Vpr via transduction. Unfortunately, these cells were unable to thrive as the Vpr protein is known to cause G2 cycle arrest. A doxycycline-inducible system was of interest, as it would potentially allow for limited expression of Vpr, yet despite many attempts it was regrettably unsuccessful during this study.

After analyzing obtained data it became apparent that although various markers were utilized with the goal of characterizing the whole extracellular vesicle populations, a large proportion of vesicles were negative for any of the chosen markers. This limitation is possibly the result of surface algorithms created to detect positive puncta. Such algorithms created for each channel of interest have been applied to thousands of extracellular vesicles with background levels derived from the secondary antibody only controls. Quite possibly during the analysis, the detection methods utilized were too conservative excluding positive puncta. Alternatively, is would be of interest to include a broader range of both integral, as well as transmembrane proteins for further characterization of the extracellular vesicle population. Perhaps, the inclusion of heat shock proteins or membrane transport proteins may better reveal the true characteristics of all extracellular vesicles obtained.

In future studies involving extracellular vesicles containing HIV-1 proteins, it would be revealing to expose neuronal cell lines to each extracellular vesicle population individually (Nef,

Tat, or Vpr) to determine their deleterious effects. Quite possibly one protein is more neurotoxic than the next or even one pathway of extracellular vesicle biogenesis produces more neurotoxic vesicles. To begin to address the latter, future studies may utilize various pharmacological treatments to inhibit one or more extracellular vesicle biogenesis pathways. For instance, Bafilomycin A1 may be utilized to inhibit the production of lysosomes or MG132 to perturb the formation of autophagosome, thus altering pathways of cellular degradation and vesicle biogenesis.

Additionally, it would be meaningful to determine how prevalent Nef, Tat or Vpr are among the entire vesicle population released from HIV-1 infected cells. Possibly as a result of HIV-1 infection, the extracellular vesicle populations are altered even more so than during the single protein expression induced here. To analyze the population of extracellular vesicles released following HIV-1 infection would require a reliable method of separating virus from extracellular vesicles. Physical and chemical characteristics, as well as biogenesis pathways are almost identical between extracellular vesicles and virions causing an analysis such as this very challenging.

In this thesis of, THE NOVEL CHARACTERIZATION OF EXTRACELLULAR VESICLES CONTAINING PROTEINS WHICH HAVE BEEN IMPLICATED IN THE PATHOGENESIS OF HIV ASSOICIATED NEUROCOGNITIVE DISORDERS we have shown that extracellular vesicles containing HIV-1 proteins are not of a homogeneous population. Through the utilization of canonical markers and wide-field deconvolution microscopy we can analyze the larger population at the single vesicle level to determine their possible mode of biogenesis. This study

provides the foundation in characterizing and better understanding extracellular vesicles which may be responsible for the pathogenesis of a multitude of neuropathological disorders.

REFERENCE LIST

1. Heaton, R.K., et al., HIV-associated neurocognitive disorders persist in the era of potent antiretroviral therapy: CHARTER Study. Neurology, 2010. 75(23): p. 2087-96.

2. Heaton, R.K., et al., HIV-associated neurocognitive disorders before and during the era of combination antiretroviral therapy: differences in rates, nature, and predictors. J Neurovirol, 2011. 17(1): p. 3-16.

3. Vivithanaporn, P., et al., Neurologic disease burden in treated HIV/AIDS predicts survival: a population- based study. Neurology, 2010. 75(13): p. 1150-8.

4. Kieffer, T.L., et al., Genotypic analysis of HIV-1 drug resistance at the limit of detection: virus production without evolution in treated adults with undetectable HIV loads. J Infect Dis, 2004. 189(8): p. 1452-65.

5. Evering, T.H., et al., Absence of HIV-1 evolution in the gut-associated lymphoid tissue from patients on combination antiviral therapy initiated during primary infection. PLoS Pathog, 2012. 8(2): p. e1002506.

6. Freeman, D., et al., Alpha-synuclein induces lysosomal rupture and cathepsin dependent reactive oxygen species following endocytosis. PLoS One, 2013. 8(4): p. e62143.

7. Mocchetti, I., A. Bachis, and V. Avdoshina, Neurotoxicity of human immunodeficiency virus-1: viral proteins and axonal transport. Neurotox Res, 2012. 21(1): p. 79-89.

8. Lindl, K.A., et al., HIV-associated neurocognitive disorder: pathogenesis and therapeutic opportunities. J Neuroimmune Pharmacol, 2010. 5(3): p. 294- 309.

9. Aqil, M., et al., Transcriptomic Analysis of mRNAs in Human Monocytic Cells Expressing the HIV-1 Nef Protein and Their Exosomes. Biomed Res Int, 2015. 2015: p. 492395.

10. Aqil, M., et al., The HIV Nef protein modulates cellular and exosomal miRNA profiles in human monocytic cells. J Extracell Vesicles, 2014. 3.

11. Hu, G., et al., Exosome-mediated shuttling of microRNA-29 regulates HIV Tat and morphine-mediated neuronal dysfunction. Cell Death Dis, 2012. 3: p. e381.

12. Hubert, A., et al., Elevated abundance, size and microRNA content of plasma extracellular vesicles in viremic HIV-1+ patients: correlations with known markers of disease progression. J Acquir Immune Defic Syndr, 2015.

13. Kadiu, I., et al., Biochemical and biologic characterization of exosomes and microvesicles as facilitators of HIV-1 infection in macrophages. J Immunol, 2012. 189(2): p. 744-54.

14. Madison, M.N. and C.M. Okeoma, Exosomes: Implications in HIV-1 Pathogenesis. Viruses, 2015. 7(7): p. 4093-118.

15. Danzer, K.M., et al., Exosomal cell-to-cell transmission of alpha synuclein oligomers. Mol Neurodegener, 2012. 7(1): p. 42.

16. Fevrier, B., et al., Cells release prions in association with exosomes. Proc Natl Acad Sci U S A, 2004. 101(26): p. 9683-8.

17. Kalani, A., et al., Exosomes: mediators of neurodegeneration, neuroprotection and therapeutics. Mol Neurobiol, 2014. 49(1): p. 590-600.

18. Rajendran, L., et al., Alzheimer's disease beta-amyloid peptides are released in association with exosomes. Proc Natl Acad Sci U S A, 2006. 103(30): p. 11172-7.

19. Nuschke A, et al., Human mesenchymal stem cells/multipotent stromal cells consume accumulated autophagosomes early in differentiation. Stem Cell Research & Therapy. 2014;5(6):140. doi:10.1186/scrt530.

20. Van der Pol, Edwin et al., (2012). Classification, Functions, and Clinical Relevance of Extracellular Vesicles. Pharmacological reviews. 64. 676-705. 10.1124/pr.112.005983.

21. Nilsson, Per & Saido, Takaomi. (2014). Dual roles for autophagy: Degradation and secretion of Alzheimer's disease Aβ peptide. BioEssays. 36. .

22. Arold, Stefan T. & Baur, Andreas S. (2001). Dynamic Nef and Nef dynamics: how structure could explain the complex activities of this small HIV protein. TRENDS in Biochemical Sciences. Vol. 26 (6) p. 356-363.

23. Saylor, Deanna, et al., HIV-associated neurocognitive disorder pathogenesis and prospects for treatment. Nature reviews. Neurology, April 2016, Vol.12(4), pp.234-48.

24. Ravi Manjithaya, Suresh Subramani, Autophagy: a broad role in unconventional protein secretion?, In Trends in Cell Biology, Volume 21, Issue 2, 2011, Pages 67-73.

25. Jovic, Marko et al. The Early Endosome: A Busy Sorting Station for Proteins at the Crossroads. Histology and histopathology. 25.1 (2010): 99–112.

26. Cohen, Myron S. et al. Acute HIV-1 Infection. The New England journal of medicine. 364.20 (2011): 1943–1954.

27. Fanales-Belasio, Emanuele, et al., HIV virology and pathogenetic mechanisms of infection: a brief overview. Annali dell'Istituto Superiore di Sanità, 2010. *46*(1), 5-14.

28. Kowal, Joanna, et al., Proteomic comparison defines novel markers to characterize heterogeneous populations of extracellular vesicle subtypes. PNAS, 2016. 113(8):968-977.

29. Powner, Dale, et al., Tetraspanin CD9 in cell migration. Biochemical Society Transactions, 2011. 39(2) p. 563-567.

30. James, Tony, et al., Defining the Roles for Vpr in HIV-1 Associated Neuropathogenesis. Journal of neurvirology. 22.4 (2016). P. 403-415.

31. Li, Ming et al. Quantitative Proteomic Analysis of Exosomes from HIV-1 Infected Lymphocytic Cells. Proteomics 12.13 (2012).

32. Kogan, Michael, and Jay Rappaport. HIV-1 Accessory Protein Vpr: Relevance in the Pathogenesis of HIV and Potential for Therapeutic Intervention. Retrovirology 8 (2011): 25.

33. Menzies, F.M., Fleming, A., and Rubinsztein, D.C., Compromised autophagy and neurodegenerative diseases. Nat Rev Neurosci, 2015. 16(6): p. 345-57.

34. Guo, J.L. and Lee, V.M., Cell-to-cell transmission of pathogenic proteins in neurodegenerative diseases. Nat Med, 2014. 20(2): p. 130-8.

35. Raposo G[1], Stoorvogel W. Extracellular vesicles: exosomes, microvesicles, and friends. J Cell Biol. 2013 Feb 18;200(4):373-83. doi: 10.1083/jcb.201211138.

36. Abels, E.R., et al., Introduction to Extracellular Vesicles: Biogenesis, RNA Cargo Selection, Content, Release, and Uptake Cell Mol Neurobiol (2016) 36: 301.

37. Gyo¨rgy B, Szabo´ TG, Pa´szto´i M et al (2011) Membrane vesicles, current state-of-the-art: emerging role of extracellular vesicles. Cell Mol Life Sci 68:2667–2688.

38. Grant BD, Donaldson JG (2009) Pathways and mechanisms of endocytic recycling. Nat Rev Mol Cell Biol 10:597–608. doi:10. 1038/nrm2755

39. Simons M[1], Raposo G. Exosomes--vesicular carriers for intercellular communication. Curr Opin Cell Biol. 2009 Aug;21(4):575-81.

40. Conde-Vancells J, Rodriguez-Suarez E, Embade N et al (2008) Characterization and comprehensive proteome profiling of exosomes secreted by hepatocytes. J Proteome Res 7:5157–5166. doi:10.1021/pr8004887

41. Colombo M, Moita C, van Niel G et al (2013) Analysis of ESCRT functions in exosome biogenesis, composition and secretion highlights the heterogeneity of extracellular vesicles. J Cell Sci 126:5553–5565. doi:10.1242/jcs.128868

42. Guduric-Fuchs J, O'Connor A, Camp B et al (2012) Selective extracellular vesicle-mediated export of an overlapping set of microRNAs from multiple cell types. BMC Genom 13:357. doi:10.1186/1471-2164-13-357

43. Jenjaroenpun P, Kremenska Y, Nair VM et al (2013) Characterization of RNA in exosomes secreted by human breast cancer cell lines using next-generation sequencing. PeerJ 1:e201. doi:10.7717/ peerj.201

44. Huang X, Yuan T, Tschannen M et al (2013) Characterization of human plasma-derived exosomal RNAs by deep sequencing. BMC Genom 14:319. doi:10.1186/1471-2164-14-319

45. Pols MS, Klumperman J (2009) Trafficking and function of the tetraspanin CD63. Exp Cell Res 315:1584–1592

46. Keller S, Sanderson MP, Stoeck A, Altevogt P (2006) Exosomes: from biogenesis and secretion to biological function. Immunol Lett 107:102–108. doi:10.1016/j.imlet.2006.09.005

47. Kramer-Albers EM, Bretz N, Tenzer S, Winterstein C, Mobius W, Berger H, Nave KA, Schild H, Trotter J (2007) Oligodendrocytes secrete exosomes containing major myelin and stress protective proteins: trophic support for axons? Proteomics Clin Appl 1:1446–1461. doi:10.1002/prca.200700522

48. Morelli AE, Larregina AT, Shufesky WJ et al (2004) Endocytosis, intracellular sorting, and processing of exosomes by dendritic cells. Blood 104:3257–3266. doi:10.1182/blood-2004-03-0824

49. Stoorvogel W, Strous GJ, Geuze HJ et al (1991) Late endosomes derive from early endosomes by maturation. Cell 65:417–427. doi:10.1016/0092-8674(91)90459-C

50. Henne WM, Buchkovich NJ, Emr SD (2011) The ESCRT pathway. Dev Cell 21:77–91

51. Raiborg C, Stenmark H (2009) The ESCRT machinery in endosomal sorting of ubiquitylated membrane proteins. Nature 458:445– 452. doi:10.1038/nature07961

52. Tamai K, Tanaka N, Nakano T et al (2010) Exosome secretion of dendritic cells is regulated by Hrs, an ESCRT-0 protein. Biochem Biophys Res Commun 399:384–390. doi:10.1016/j. bbrc.2010.07.083

53. Shields SB, Oestreich AJ, Winistorfer S et al (2009) ESCRT ubiquitin-binding domains function cooperatively during MVB cargo sorting. J Cell Biol 185:213–224. doi:10.1083/jcb. 200811130

54. Babst M, Katzmann DJ, Estepa-Sabal EJ et al (2002) ESCRT-III: an endosome-associated heterooligomeric protein complex required for MVB sorting. Dev Cell 3:271–282. doi:10.1016/S1534- 5807(02)00220-4

55. Dengjel, J., Høyer-Hansen, M., Nielsen, M. O., Eisenberg, T., Harder, L. M., Schandorff, S., et al. (2012). Identification of autophagosome-associated proteins and regulators by quantitative proteomic analysis and genetic screens. Mol. Cell.

56. Rabouille C, et al. Diversity in unconventional protein secretion. J Cell Sci. 2012; 125:5251–5255. [PubMed: 23377655]

57. Rubartelli A, et al. A novel secretory pathway for interleukin-1 beta, a protein lacking a signal sequence. The EMBO journal. 1990; 9:1503–1510. [PubMed: 2328723]

58. Muesch A, et al. A novel pathway for secretory proteins? Trends Biochem Sci. 1990; 15:86–88. [PubMed: 2139259]

59. Piccioli P, Rubartelli A. The secretion of IL-1beta and options for release. Semin Immunol. 2013; 25:425–429. [PubMed: 24201029]

60. Kaushik S, Cuervo AM. 2012. Chaperone-mediated autophagy: a unique way to enter the lysosome world. Trends Cell Biol. 22:407–17

61. Li WW, Li J, Bao JK. 2012. Microautophagy: lesser-known self-eating. Cell Mol. Life Sci. 69:1125–36

62. Lamb CA, Yoshimori T, Tooze SA. 2013. The autophagosome: origins unknown, biogenesis complex. Nat. Rev. Mol. Cell Biol. 14:759–74

63. Hara T, Takamura A, Kishi C, Iemura S, Natsume T, et al. 2008. FIP200, a ULK-interacting protein, is required for autophagosome formation in mammalian cells. J. Cell Biol. 181:497–510

64. Jung CH, Jun CB, Ro SH, Kim YM, Otto NM, et al. 2009. ULK-Atg13-FIP200 complexes mediate mTOR signaling to the autophagy machinery. Mol. Biol. Cell 20:1992–200

65. Kim J, Kundu M, Viollet B, Guan KL. 2011. AMPK and mTOR regulate autophagy through direct phosphorylation of Ulk1. Nat. Cell Biol. 13:132–41

66. Geng J, Klionsky DJ (2008) The Atg8 and Atg12 ubiquitin-like conjugation systems in macroautophagy. 'Protein modifications: beyond the usual suspects' review series. EMBO Rep 9(9):859–864

67. Mizushima N, Noda T, Yoshimori T, Tanaka Y, Ishii T, George MD, Klionsky DJ, Ohsumi M, Ohsumi Y (1998) A protein conjugation system essential for autophagy. Nature 395(6700):395–398

68. Stolz A, Ernst A, Dikic I (2014) Cargo recognition and trafficking in selective autophagy. Nat Cell Biol 16(6):495–501

69. Kaufmann A, Beier V, Franquelim HG, Wollert T (2014) Molecular mechanism of autophagic membrane-scaffold assembly and disassembly. Cell 156(3):469–481.

70. Fujita N, Itoh T, Omori H, Fukuda M, Noda T, Yoshimori T (2008) The Atg16L complex specifies the site of LC3 lipidation for membrane biogenesis in autophagy. Mol Biol Cell 19(5):2092–2100

71. Fader, C. M., and Colombo, M. I. (2009) Autophagy and multivesicular bodies: two closely related partners. Cell Death Differ. 16, 70–78

72. Xie, Z., and Klionsky, D. J. (2007) Autophagosome formation: core machinery and adaptations. Nat. Cell Biol. 9, 1102–1109

73. Mehrpour, M., Esclatine, A., Beau, I., and Codogno, P. (2010) Overview of macroautophagy regulation in mammalian cells. Cell 20, 748–762

74. Tooze, S. A., and Yoshimori, T. (2010) The origin of the autophagosomal membrane. Nat. Cell Biol. 12, 831–835

75. Mizushima N, et al. The role of Atg proteins in autophagosome formation. Annu Rev Cell Dev Biol. 2011; 27:107–132. [PubMed: 21801009]

76. Rogov V, et al. Interactions between autophagy receptors and ubiquitin-like proteins form the molecular basis for selective autophagy. Mol Cell. 2014; 53:167–178. [PubMed: 24462201]

77. Galluzzi L, et al. Metabolic Control of Autophagy. Cell. 2014; 159:1263–1276. [PubMed: 25480292]

78. Ganley IG, Lam du H, Wang J, Ding X, Chen S, Jiang X. ULK1.ATG13.FIP200 complex mediates mTOR signaling and is essential for autophagy. J Biol Chem. 2009;284(18):12297–12305.

79. Hosokawa N, et al. Nutrient-dependent mTORC1 association with the ULK1-Atg13-FIP200 complex required for autophagy. Mol Biol Cell. 2009;20(7):1981–1991.

80. R. L. Vidal, S. Matus, L. Bargsted, C. Hetz, Targeting autophagy in neurodegenerative diseases. Trends Pharmacol. Sci. 35, 583–591 (2014).

81. Dupont N, et al. Autophagy-based unconventional secretory pathway for extracellular delivery of IL-1beta. EMBO J. 2011; 30:4701–4711. [PubMed: 22068051]

82. Bruns C, et al. Biogenesis of a novel compartment for autophagosome-mediated unconventional protein secretion. The Journal of cell biology. 2011; 195:979–992. [PubMed: 22144692]

83. Liou, W.; Geuze, H.J.; Geelen, M.J.; Slot, J.W. The autophagic and endocytic pathways converge at the nascent autophagic vacuoles. J. Cell Biol. 1997, 136, 61–70.

84. Berg, T.O.; Fengsrud, M.; Stromhaug, P.E.; Berg, T.; Seglen, P.O. Isolation and characterization of rat liver amphisomes. Evidence for fusion of autophagosomes with both early and late endosomes. J. Biol. Chem. 1998, 273, 21883–21892

85. Fader CM, Sanchez D, Furlan M, Colombo MI: Induction of autophagy promotes fusion of multivesicular bodies with autophagic vacuoles in k562 cells. Traffic 2008, 9(2):230–250.

86. Nixon, R.A. The role of autophagy in neurodegenerative disease. Nat. Med. 2013, 19, 983–997.

87. Saribas, A Sami, et al., Dysregulation of Autophagy by HIV-1 Nef in Human Astrocytes. Cell Cycle 14.18 (2015): 2899–2904.

88. Peng, Jinsong, et al., The HIV-1 transgenic rat as a model for HIV-1 infected individuals on HAART. Journal of Neuroimmunology Vol 218 (2010): 94-101.

89. Hui, Liang et al. Role of Endolysosomes in HIV-1 Tat-Induced Neurotoxicity. ASN NEURO 4.4 (2012)

90. Rohrbach, J., et al., Cellular immune responses to HCV core increase and HCV RNA levels decrease during successful antiretroviral therapy Gut 2010; 59: 1252-1258.

91. Gonzalez, M. The HIV-1 Vpr Protein: A Multifaceted Target for Therapeutic Intervention. International Journal of Molecular Sciences (2017). Vol. 18(1).

92. Li, Pin et al. Progress in Exosome Isolation Techniques. Theranostics 7.3 (2017): 789–804.

VITA

The author, Grace Ispas, was born in Munster, Indiana on October 22, 1991 to Jeffrey and Vicki Ispas. She attended Goshen College in Goshen, Indiana where she earned her Bachelor's of Arts in Biological and Psychological Sciences in May 2014. In 2015, Grace matriculated into the Loyola University Chicago Stritch School Infectious Disease and Immunology Graduate Program and joined the laboratory of Dr. Ed Campbell.

Following graduation, Grace is looking forward to spending more time with her eight month old daughter Arya.